Drawing Pressure Estimation Using Torque Feedback Control Model of A 4-DOF Robotic Arm

Meng Cheng Lau[1], Chi-Tai Cheng[2], Jacky Baltes[3], and John Anderson[3]

[1] Center for Artificial Intelligence Technology, Universiti Kebangsaan Malaysia, 43600 Bangi, Selangor, Malaysia
[2] Department of Electrical Engineering, Tamkang University, New Taipei City 25137, Taiwan (R.O.C.)
[3] Autonomous Agent Lab, University of Manitoba, Winnipeg, Manitoba R3T 2N2, Canada

mengcheng.lau@gmail.com,124646@mail.tku.edu.tw,{jacky,andersj}@cs.umanitoba.ca

Abstract. This paper we introduce a torque feedback control (TFC) model to estimate pressure of the hand on a 4-DOF robotic arm of Betty, a humanoid robot. Based on several preliminary experiments of different stroke patterns, we measured and analysed the torque replies of Betty's servos in order to model the torque feedback. We developed a robust humanoid system to create sketch like drawing with limited hardware which has no force sensor but basic torque feedback from servos to estimate pressure apply on drawing pad. We investigated the efficiency of using the TFC in the drawing task based on several different stroke patterns. The experimental results indicate that the TFC model successfully corrected the errors during the drawing task.

Keywords: Torque Feedback Control, Robotic Arm, Drawing Pressure Estimation

1 Introduction

In many applications [1–5], a robot must explicitly control the force it applies to the object it is manipulating, i.e., the actuators must be controlled to achieve the desired forces. Force control using feedback of joint torques is limited by the accuracy over a resistor to estimate the input current of the motors [6, 7]. This indirect measurement has several errors, including the variations in the losses in the motor itself and the gearbox. To obtain accurate control of the force vector at the end effector, a wrist force sensor is placed between the tool plate and the end effector to measure end-effector force [8–10]. The force transform from the sensor to the end effector is simple but these load cell sensors are usually expensive. Torque in joint space is controlled by controlling the torque applied by each actuator (servo). Torque can be measured using a sensor (accurate) or estimated from armature current (simple). In this paper, we proposed a torque feedback control (TFC) to provide significant feedback for pressure estimation throughout the drawing process. The evaluation will be discussed in Section 4.

2 Hardware Configuration

The upper body of Betty consists of a twelve-revolute joint system with 12 degrees of freedom (DOF). Its head has 4 DOFs which are pan, tilt, swing and one DOF for the mouth. Each of its arms provides 4 DOFs, shoulders allow lateral and frontal motions, elbow gives lateral motion and a wrist motion. These joints are constructed by four Dynamixel RX-64 servos in the head and four Dynamixel RX-64 servos for each of its arms. Fig.1 shows the overview of Betty's upper body.

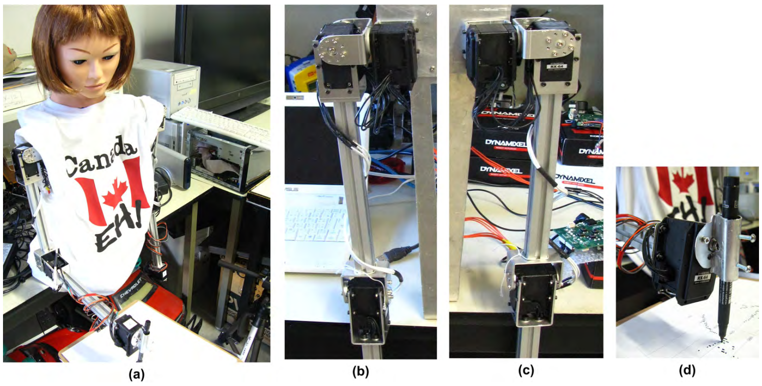

Fig. 1: Overview of Betty's 12-DOF upper body.

The main reason we chose RX-64 to construct Betty's arms is it has higher final maximum holding torque, 64.4∼77.2 kgf.cm compared to only 12∼16.5 kgf.cm for the AX-12 [11, 12] which were used in Betty's previous design [13, 14]. This improvement allows the RX-64 servos to generate sufficient torque to support the weight of Betty's arms and head. In order to control the servos, we use Dynamixel's dedicated controller, CM-2+ from Robotis as the central control unit with its `AVR ATmega128` microcontroller. The real-time OS establishes communication with the servos and its implementation can be seen in our previous publications [13, 14].

3 Torque Feedback Control (TFC) model

For Dynamixel RX-64 servos, torque can be measured on a 0-1023 (0x3FF) scale, based on its maximum holding (stall) torque 64 kgf-cm (6.92 Nm) at 18V. As seen in Tira-Thompson's [15] study, a Dynamixel servo can read back the current position, temperature, load (torque), etc.. For instance, position read back can measures to within 0.5 degrees of accuracy at full communication speed in every 130ms. However, reading the present load would not provide precise torque measurement. Robotis posted a comment on their official website that the “Present Load” or torque measurement is not a real torque or electrical current measurement. It is actually just based on the difference between current position and goal position. It has a control loop to make sure the motor actually got to the goal position. Hence, the “Present Load” value is the torque that the servo is *applying*, not the torque that it is *experiencing*. Therefore, it is not possible to perform “Torque Control” of a servo [16].

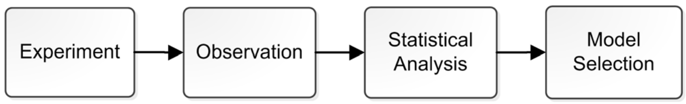

Fig. 2: Designing of torque feedback control (TFC) model.

However, in the brief tutorial book of Anderson [17], he suggested the reality can be estimated based on the empirical evidence hypotheses and statistical models. In our approach, we designed a simple torque feedback control (TFC) model based on two simplest strokes, horizontal and vertical. Some preliminary experiments are performed to obtain suitable sets of data from servos' torque feedback (right arm). By using this data, a simple TFC model is created and the suitable set of candidate models is selected based on statistical hypothesis testing to estimate stroke pressure. “Given candidate models of similar predictive or explanatory power, the simplest model is most likely to be correct” [17]. Fig.3 shows the design of Betty's TFC model.

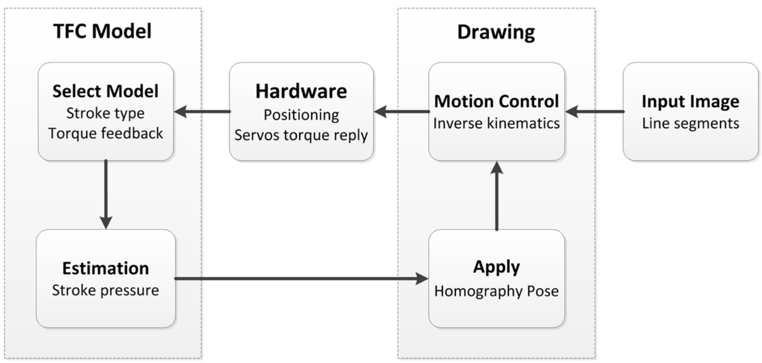

Fig. 3: Processing flow of torque feedback control (TFC) for drawing task.

This TFC approach is implemented to observe pen pressure during the drawing process to prevent overpressure or no-touch errors. Several experiments were conducted to obtain the statistical model. It provides optimum thresholds to estimate pen pressure. In these experiments, the pressure applied on the Wacom Bamboo tablet (underneath the paper) are recorded.

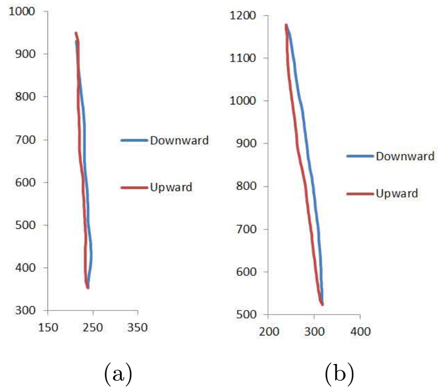

Fig. 4: (a):Medium pressure vertical strokes and (b): High pressure vertical strokes.

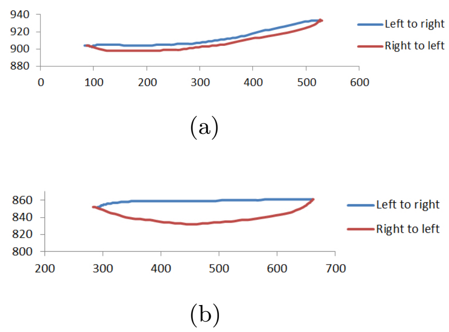

Fig. 5: (a):Medium pressure horizontal strokes and (b): High pressure horizontal strokes.

3.1 Experimental Setup

Fig.6 shows the experimental setup of Betty and the drawing pad. During the experiments, Betty used its right arm to draw based on sinusoidal interpolation motion trajectory. We placed a Wacom Bamboo tablet (CTH670M) under the paper to measure position and pressure on the drawing pad. The measures of tablet were only used to established the reliability of the experiments but did not provide any feedback control to Betty. The drawing area is based on the specification provided by the manufacturer, the accuracy of the tablet is ± 0.5 mm on a 217 mm x 137 mm active area [18]. For each experimental trial, we recorded the 0 to 1024 pressure level on the tablet within the scale of 0.00 to 1.00.

3.2 Preliminary Experiments

In this experiment, we established the tests for torque reliability. Betty's right arm performed two basic stroke types are, namely vertical and horizontal strokes. Two direction are drawn for both type of strokes which are upward-downward and left-right. Fig.4 shows the average vertical strokes and Fig.5 shows the average horizontal strokes from 100 recorded strokes respectively in different directions. Medium pressure is the normal pressure read from the tablet in the

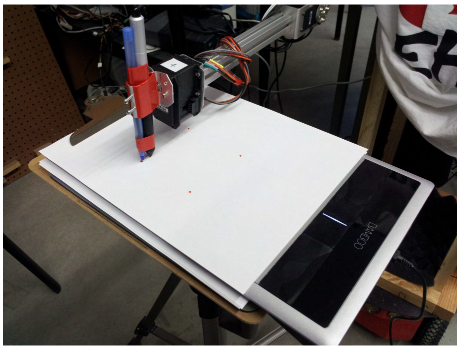

Fig. 6: Experimental setup using a CTH640M tablet, Betty, and pen.

range of 0.7 ± 0.1 and high pressure represents 1.0 (highest) pressure measurement from the tablet. From these preliminary experiments we observed that high pressure caused significant errors in both horizontal and vertical strokes compares to normal pressure. So, it makes the estimation of stroke pressure essential. We recorded the torque measurements of each servos on Betty's right arm. By using this torque data as seen in the following tables, a simple TFC model is created. Hence, the suitable set of candidate models can be selected based on statistical hypothesis testing to estimate stroke pressure.

Table 1 shows the torque measurements from four servos on the right arm namely ID 1, 2, 3 and 4 for shoulder-frontal, shoulder-lateral, elbow and wrist respectively. Table 2 shows the model of vertical downward stroke which suggests how significant torque measurements are affected by different stroke pressure. As seen in Table 2, servo ID 2 is not significant to differentiate normal pressure stroke from no-touch conditions. However, servos ID 1 and 3 torques are highly significant to be used as the evaluators to estimate the pen's tip pressure for this stroke pattern.

Table 1: Results of vertical stroke (downward) tests.

Vertical Strokes (Downward)												
Average Pressure	**No**				**0.67**				**1.00**			
Servo ID	1	2	3	4	1	2	3	4	1	2	3	4
Average	16.88	0.02	52.42	0.12	32.32	0.84	20.7	23.6	200.44	11.82	93.1	1.42
Std. Dev.	12.21	0.14	7.65	0.33	16.24	5.37	8.95	2.83	12.13	7.01	8.92	4.36

Table 2: Comparison of vertical (downward) stroke model.

	Servo ID			
Pressure Comparison	**1**	**2**	**3**	**4**
No vs. Normal	**2.96e-07**	*0.1430*[1]	**1.24e-34**	3.59e-48
No vs High	**6.73e-89**	2.26e-16	**2.65e-43**	0.0202
Normal vs. High	**3.27e-74**	4.05e-14	**2.57e-63**	3.41e-47

[1] Not significant to identify different pressure on pen tip.

Table 3 and Table 4 show the model of vertical upward stroke. As seen in Table 4, servo ID 2 has no significant difference between normal pressure stroke and no-touch conditions. But servos ID 1, 3 and 4 torques are highly significant to be considered as the evaluators to estimate the pen's tip pressure for vertical upward stroke.

Table 3: Results of vertical stroke (upward) tests.

Vertical Strokes (Upward)												
Average Pressure	**No**				**0.67**				**1.00**			
Servo ID	1	**2**	3	4	1	**2**	3	4	1	2	3	4
Average	76.04	0.12	33.36	0.2	32.42	1.08	11.96	23.52	40.96	58.58	46.42	18.78
Std. Dev.	11.65	0.33	6.08	0.4	18.22	3.99	10.12	3.39	3.08	18.42	8.34	5.21

Table 4: Comparison of vertical stroke (upward) model.

	Servo ID			
Pressure Comparison	**1**	**2**	**3**	**4**
No vs. Normal	**2.25e-24**	*0.048072*[1]	**2.08e-21**	**3.81e-44**
No vs High	**4.90e-28**	**9.74E-28**	**2.32e-14**	**3.67e-30**
Normal vs. High	0.000964	**2.19e-28**	**1.31e-33**	3.20e-07

[1] Not significant to identify different pressure on pen tip.

Table 5 and Table 6 show the model of horizontal right-left stroke. As seen in Table 6, it is not identical to the previous stroke types we discussed. For horizontal right-left stroke, servo ID 1 is not significantly different to identify high pressure stroke and no-touch conditions. However, it is highly significant to differentiate these conditions from normal pressure. Servos ID 3 and 4 torques are also highly significant to be used as the evaluators to estimate the pen's tip pressure.

Table 5: Results of horizontal stroke (left to right) tests.

Horizontal Strokes (Left to right)												
Average Pressure	**No**				**0.67**				**1.00**			
Servo ID	**1**	2	3	4	1	2	3	4	**1**	2	3	4
Average	47.26	30.04	66.24	26.52	23.64	36.34	21.86	23.06	47.44	54.74	41.02	11.66
Std. Dev.	7.77	12.87	7.76	4.68	1.79	14.99	4.04	5.41	2.55	12.12	3.18	5.82

Table 6: Comparison of horizontal stroke (left to right) model.

	Servo ID			
Pressure Comparison	**1**	**2**	**3**	**4**
No vs. Normal	**5.90E-28**	0.013217	**9.69E-49**	0.00046
No vs High	*0.438413*[1]	**1.15E-16**	**2.76E-31**	**3.77E-25**
Normal vs. High	1.56E-69	6.08E-10	**3.48E-45**	**3.05E-17**

[1] Not significant to identify different pressure on pen tip.

Table 7 and Table 8 show the model of horizontal right-left stroke. As seen in Table 8, servo ID 2 is not significant to differentiate normal pressure stroke from no-touch conditions like the other vertical strokes we have seen. Similar to vertical upward stroke, servos ID 1, 3 and 4 torques are highly significant to be used as the evaluators to estimate the pen's tip pressure for horizontal right-left stroke.

Table 7: Results of horizontal stroke (right to left) test.

Horizontal Strokes (Right to left)												
Average Pressure	**No**				**0.67**				**1.00**			
Servo ID	1	**2**	3	4	1	**2**	3	4	1	2	3	4
Average	45.14	35.34	66.24	26.36	18.52	35.56	20.84	17.06	25.72	11.88	88.86	1.06
Std. Dev.	6.55	15.14	7.76	6.62	4.21	13.84	4.1	5.45	14.91	7.07	13.83	3.82

Table 8: Comparison of horizontal stroke (right to left) model.

	Servo ID			
Pressure Comparison	**1**	**2**	**3**	**4**
No vs. Normal	**8.33e-40**	*0.469855*[1]	**1.33e-49**	**7.56e-12**
No vs High	**1.94e-12**	2.95e-15	**4.88e-16**	**2.03e-37**
Normal vs. High	0.000871	**4.93e-17**	**1.25e-39**	**7.85e-30**

[1] Not significant to identify different pressure on pen tip.

Based on these preliminary experiments, Table 9 shows the general TFC model to estimate the pen's tip pressure from servos' torque feedback. For simplicity of the implementation Servo ID 1 and 3 (shoulder and elbow) are mostly used. Fig.7 illustrates the control loop of the TFC model. It showed that by way of different stroke patterns, a significant difference in torque feedback can be measured. It allowed for a significant estimate of the pressure of the pen's tip.

Table 9: Torque feedback control model.

Stroke Type	Torque (τ_i) threshold conditions for normal pressure	
	Low Pressure (No-touch)	High Pressure
Vertical downward	ID1: $\tau_1 < 25$	ID1: $\tau_1 > 50$
Vertical upward	ID1: $\tau_1 > 50$	ID1: $\tau_1 < 50$ and ID3: $\tau_3 > 40$
Horizontal left-right	ID1: $\tau_1 > 30$ and ID3: $20 < \tau_3 < 35$	ID3: $\tau_3 > 20$
Horizontal right-left	ID1: $\tau_1 > 40$ and ID3: $20 < \tau_3 < 35$	ID2: $\tau_2 > 35$ and ID3: $\tau_3 > 20$

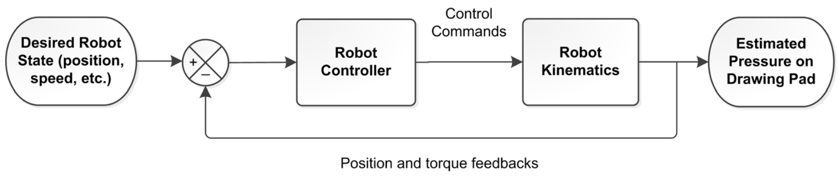

Fig. 7: Closed-loop control diagram for TFC

4 Torque Feedback Control Experiment

In the experiments, we evaluated the feasibility and efficiency of our TFC model implementation based on the generic drawing tasks. We used two initial conditions, no-touch (0.0) and high pressure (1.0) on the tablet to justify the feasibility of TFC to correct these errors. Betty repeated 30 times for each vertical (upward and downward), horizontal (left-right and right-left) and diagonal lines (left-right with downward) based on these two initial conditions with total of 150 trails. For these trials, the average pressure on the tablet and measured torque reply for each stroke were recorded. We measured the error of pressure for each stroke based on the TFC model using initial errors of "high pressure", "low pressure" (no-touch) and desired "normal pressure" as seen in Section 3.2. The ideal average "normal pressure" experience on the tablet should be at the level of 0.7±0.1. A correction of 10 mm was applied when the measured torque was too low or too high. The total number of required correcting strokes to finish a drawing task and the changes in error over time, were sampled at some defined interval.

Fig.8 shows the different pressure applied to the tablet. In Fig.8(a), it started with initial lower pressure strokes until it was corrected by the TFC model in two strokes. Similarly, the system corrected the initial high pressure error in two

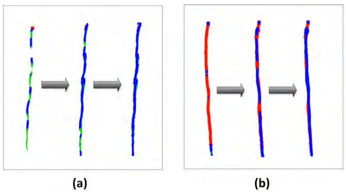

Fig. 8: Stroke pressure correction based on torque feedback control. **(a)**: low to normal **(b)**: high to normal. Green, blue and red were used to indicate low, normal and high pressure measurements respectively.

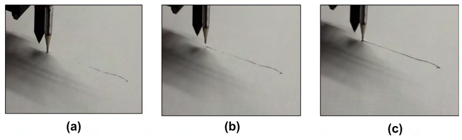

Fig. 9: Real world example of stroke pressure correction. A line segment is completed in few trial after depth correction based on torque feedback from servos.

strokes as seen in Fig.8(b). An real world example of the pressure correction is illustrated in Fig.9.

Fig.10 and 11 show how different stroke types corrected the high pressure error with their average pressures for each stroke. These figures clearly show that the high pressure error could be corrected at average of three strokes in all tested stroke types. From the 1.0 pressure recorded in the first stroke, the average of pressure detected was reduced to the 0.7±0.1 range. Fig.12 and Fig.13 show the no-touch error correction results and their average pressures for each stroke. As we have seen in the high pressure error results, the no-touch error could also be corrected at average of three strokes in those tested stroke types. From the initial no-touch stroke (no pressure is read from the tablet) the average of pressure detected increased to the 0.7±0.1 range.

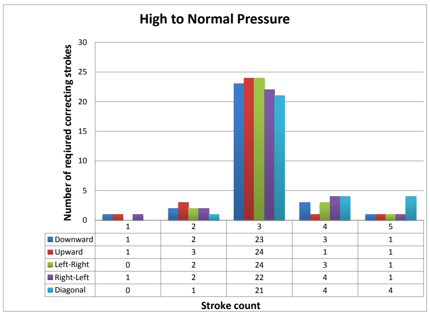

Fig. 10: Number of stroke occurrence: High to normal pressure.

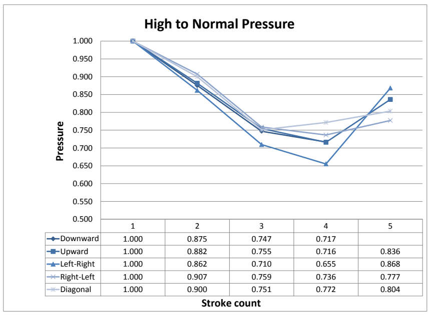

Fig. 11: Average pressure for each strokes: High to normal pressure.

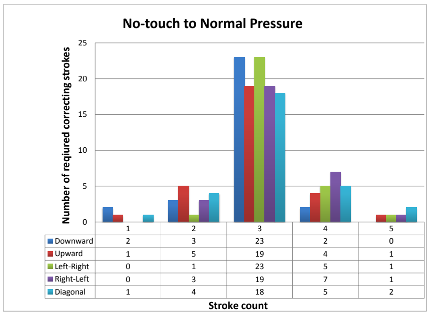

Fig. 12: Number of stroke occurrence: No-touch to normal pressure.

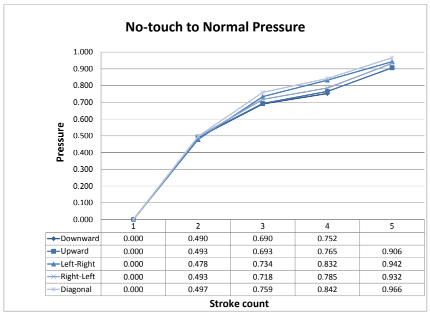

Fig. 13: Average pressure for each strokes: No-touch to normal pressure.

In this experiment, we labelled a trail as failure if no successful correction after the first stroke and the last stroke (fifth stroke). Hence, the TFC model provides 92.7% and 94.0% of successful detection of high pressure and no-touch respectively. Fig.14 shows the averages of trails needed to make the correction of each stroke type in both the high pressure and the no-touch conditions.

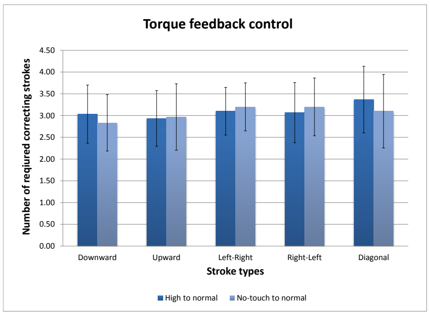

Fig. 14: Number of strokes for different stroke type based on TFC model. Error bars indicate the standard deviation.

5 Conclusion

The capability to evaluate the efficiency of different drawing implementations is very important. Unfortunately, none of the current research done in the field has provided a conclusive platform for drawing output evaluation. In our work, we used a Bamboo tablet and a series of experiments to provide the capability of drawing evaluation. This may lead to a better understanding of the various components, such as the correlation between pressure and deviation in different implementations. In this paper, we have described our methods and hardware that we used to evaluate the implementations of TFC model for a 4-DOF robotic arm. Based on the experimental results, they show that the TFC model successfully corrected the errors during the drawing task when no accurate force sensor feedback at the end effector is used. We established that TFC in the drawing task are reliable to pressure error deviation of strokes more than 90% of the time.

References

1. Kim, I.M., Kim, H.S., Song, J.B.: Design of joint torque sensor and joint structure of a robot arm to minimize crosstalk and torque ripple. In: Ubiquitous Robots and Ambient Intelligence (URAI), 2012 9th International Conference on. (Nov 2012) 404–407
2. Ott, C., Eiberger, O., Englsberger, J., Roa, M.A., Albu-Schauml;ffer, A.: Hardware and control concept for an experimental bipedal robot with joint torque sensors. Journal of the Robotics Society of Japan **30**(4) (2012) 378–382
3. Kim, T.K., Kim, D.Y., Cha, D.H., vun Choi, S., Kim, B.S., Hwang, J.H., Park, C.W.: Development of joint torque sensor and calibration method for robot finger. In: Ubiquitous Robots and Ambient Intelligence (URAI), 2013 10th International Conference on. (Oct 2013) 161–162
4. Tian, L., Goldenberg, A.: Robust adaptive control of flexible joint robots with joint torque feedback. In: Robotics and Automation, 1995. Proceedings., 1995 IEEE International Conference on. Volume 1. (may 1995) 1229 –1234 vol.1
5. Zhang, G., Furusho, J.: Control of robot arms using joint torque sensors. Control Systems, IEEE **18**(1) (feb 1998) 48 –55
6. Luh, J., Fisher, W., Paul, R.: Joint torque control by a direct feedback for industrial robots. Automatic Control, IEEE Transactions on **28**(2) (feb 1983) 153 – 161
7. Aghili, F., Buehler, M., Hollerbach, J.M.: Dynamics and control of direct-drive robots with positive joint torque feedback. In: Proceeding of IEEE Internatinal Conference Robotics and Automation. (1997) 2865–2870
8. Leite, A.C., Lizarralde, F., Hsu, L.: Hybrid adaptive vision-force control for robot manipulators interacting with unknown surfaces. Int. J. Rob. Res. **28**(7) (July 2009) 911–926
9. Baeten, J., de Schutter, J., Schutter, J.: Integrated Visual Servoing and Force Control: The Task Frame Approach. Engineering online library. Springer (2004)
10. Olsson, T., Bengtsson, J., Johansson, R., Malm, H.: Force control and visual servoing using planar surface identification. In: Proceedings of the 2002 IEEE International Conference on Robotics & Automation, Washington, DC, IEEE (May 2002) 4211–4216
11. Robotis: Robotis: User's manual dynamixel rx-64 (2007)
12. Robotis: Robotis: User's manual dynamixel ax-12 (2006)
13. Lau, M.C., Baltes, J.: The real-time embedded system for a humanoid: Betty. In: Proceedings of the 13th FIRA Robot World Congress. Volume 103 of Communications in Computer and Information Science., Bangalore, India, Springer-Verlag Berlin Heidelberg (September 2010) 122–129

14. Baltes, J., Cheng, C.T., Lau, M.C., Anderson, J.E.: Cost oriented automation approach to upper body humanoid robot. In: Proceedings of the 18th IFAC World Congress, Milano, Italy (September 2011)
15. Tira-Thompson, E.: Digital servo calibration and modeling. Technical Report CMU-RI-TR-09-41, Robotics Institute, Pittsburgh, PA (March 2009)
16. Emami, S.: Dynamixel servo motors. http://www.shervinemami.info/dynamixels.html (2009) Accessed: 2011-11-20.
17. Anderson, D.: Model Based Inference in the Life Sciences: A Primer on Evidence. Springer Science + Business Media (2008)
18. Futureshop: Wacom bamboo create tablet (cth670m). http://www.futureshop.ca/en-CA/product/wacom-wacom-bamboo-create-tablet-cth670m-cth670m/10180531.aspx (2013) Accessed: 2013-10-20.